Contents lists available at ScienceDirect

Nuclear Engineering and Technology

journal homepage: www.elsevier.com/locate/net

Original Article

Serial line multiplexing method based on bipolar pulse for PET

Yeonkyeong Kim [a], Yong Choi [a, *], Kyu Bom Kim [b, **], Hyuntae Leem [a], Jin Ho Jung [a]

[a] Molecular Imaging Research & Education (MiRe) Laboratory, Department of Electronic Engineering, Sogang University, Seoul, Republic of Korea
[b] Department of Integrative Medicine, Major in Digital Healthcare, Yonsei University, Seoul, Republic of Korea

ARTICLE INFO

ABSTRACT

Although the individual channel readout method can improve the performance of PET detectors with pixelated photo-sensors, such as silicon photomultiplier (SiPM), this method leads to a significant increase in the number of readout channels. In this study, we proposed a novel multiplexing method that could effectively reduce the number of readout channels to reduce system complexity and development cost. The proposed multiplexing circuit was designed to generate bipolar pulses with different zero-crossing points by adjusting the time constant of the high-pass filter connected to each channel of a pixelated photo-sensor. The channel position of the detected gamma-ray was identified by estimating the width between the rising edge and the zero-crossing point of the bipolar pulse. In order to evaluate the performance of the proposed multiplexing circuit, four detector blocks, each consisting of a 4×4 array of 3 mm $\times$ 3 mm $\times$ 20 mm LYSO and a 4×4 SiPM array, were constructed. The average energy resolution was $13.2 \pm 1.1\%$ for all 64 crystal pixels and each pixel position was accurately identified. A coincidence timing resolution was 580 ± 12 ps. The experimental results indicated that the novel multiplexing method proposed in this study is able to effectively reduce the number of readout channels while maintaining accurate position identification with good energy and timing performance. In addition, it could be useful for the development of PET systems consisting of a large number of pixelated detectors.

© 2021 Korean Nuclear Society, Published by Elsevier Korea LLC. This is an open access article under the CC BY-NC-ND license (http://creativecommons.org/licenses/by-nc-nd/4.0/).

1. Introduction

When developing a gamma-ray imaging system, such as a positron emission tomography (PET) and a gamma camera, a large number of photo-sensors are necessary. This requirement is even more prominent in modern systems with increased imaging fields of view (FOV). However, imaging systems that use many photo-sensors suffer from increased complexity of signal processing and high development costs. To overcome these problems, many research groups have been studying various multiplexing methods which can increase the multiplexing ratio with minimized performance degradation of the detector [1—7].

A resistive charge division method has been used widely because it can provide good position identification accuracy with a simple structure [8,9]. However, this method is not ideal for PET detectors applied with photo-sensors, such as silicon photo-multiplier (SiPM), because coincidence resolving time (CRT) can be degraded due to low-pass filtering effects caused by combining the resistor of the multiplexing circuit and parasitic capacitance of the SiPM [10—12].

A capacitive charge division method has been developed to improve the timing performance degradation caused by the resistive charge division method. Although the capacitive charge division method can result in improved timing resolution, it provides worse energy resolution and flood histogram quality because of the reduced amplitude and undershoot caused by the capacitors [13—16]. The two abovementioned methods based on the charge division multiplexing method have generally reduced the number of readout channels to 4—5, but as the number of channels increases, the position identification capability and other performance could decrease [17,18].

Recently, a new multiplexing method utilizing an electrical delay line has been proposed to achieve a high multiplexing ratio [19—22]. This method has the advantage of good timing performance because it does not employ passive elements. However, it

* Corresponding author. Department of Electronic Engineering, Sogang University, 35,Baekbeom-ro, Mapo-gu, Seoul, Republic of Korea.
** Corresponding author. Gangnam Severance Hospital Future Medicine Research Center, 20, 63rd Road, Unju-ro, Gangnam-gu, Seoul, Republic of Korea.
E-mail addresses: ychoi@sogang.ac.kr (Y. Choi), ssmakal@yuhs.ac (K.B. Kim), lht0898@osteosys.com (H. Leem), jinho1115@gmail.com (J.H. Jung).

would degrade the accuracy of position identification depending on the threshold level for position identification. In addition, it is difficult to apply this method to the development of large-scale systems due to its limited expandability.

In this paper, a novel multiplexing method, the serial line multiplexing method, was developed to effectively reduce the number of output channels and to provide easy expandability, for example, by 16:2 or 64:3 for SiPM-based pixelated detectors, which are widely used for PET system development. It is expected that the serial line multiplexing method will reduce the complexity of signal processing by measuring the pulse width according to the position of detected radiation for PET, which will lead to reduced development costs.

2. Materials and methods

2.1. Principle of serial line multiplexing

The principle of the serial line multiplexing method is to identify a detected position by generating and measuring a bipolar pulse that has the position of detected radiation in a PET detector. The output signals of the serial line multiplexing method consist of an anode summing output signal for position identification and a cathode summing output signal for measuring energy resolution and CRT.

To create different RC time constants for each channel position of the photo-sensor, high-pass filters (HPF) were designed using load resistors and capacitors for each anode channel of the photo-sensor, and each anode channel was connected to an anode summing output (Fig. 1). Energy and timing information was measured using the amplitude and rising time of the cathode summing output signal. Anode and cathode summing output signals from the pixelated detector were individually transmitted to the input of the preamplifier.

2.2. Simulation study

Based on the principles of the method outlined above, a SPICE simulation was performed to investigate the feasibility of the serial line multiplexing method. The simulation was used to observe the change in the pulse width of the position signal according to the HPF value of the SiPM equivalent circuit [23–26]. It was observed that the zero-crossing point values increased exponentially as HPF increased. Equation (1) was derived to find the zero-crossing point values as a function of RC:

$$\text{Zero crossing point} = A_0 - A_0 \cdot e^{\left(1 - \frac{RC}{minRC}\right)} \tag{1}$$

where A_0 represents the zero-crossing point of the last channel

Table 1
The resistor and capacitor values of HPF.

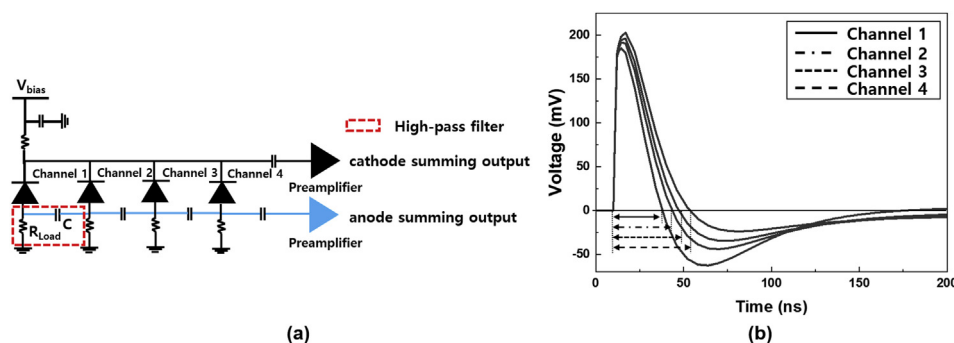| Channel	Capacitor value (nF)	Resistor value (Ω)
1	8.2	511
2	12.0	
3	10.0	
4	8.2	
5	8.2	
6	4.7	
7	4.7	
8	2.0	

with the largest pulse width and $minRC$ is the minimum RC time constant value. To determine the optimal RC time constant values of HPF in the serial line multiplexing circuit, two approaches were designed and then compared to assess their position identification accuracy. The first approach employed the same RC time constant value (RC-values (ns): 220) for all channel positions from 1 to 8. The second approach applied different RC time constant values (RC-values (ns): 346, 524, 670, 930, 1196, 1673, 2489 and 4190) to each channel position from 1 to 8. The different RC time constant values of the second approach were adjusted so that there was a difference of 20 ns between the zero-crossing point of each channel position.

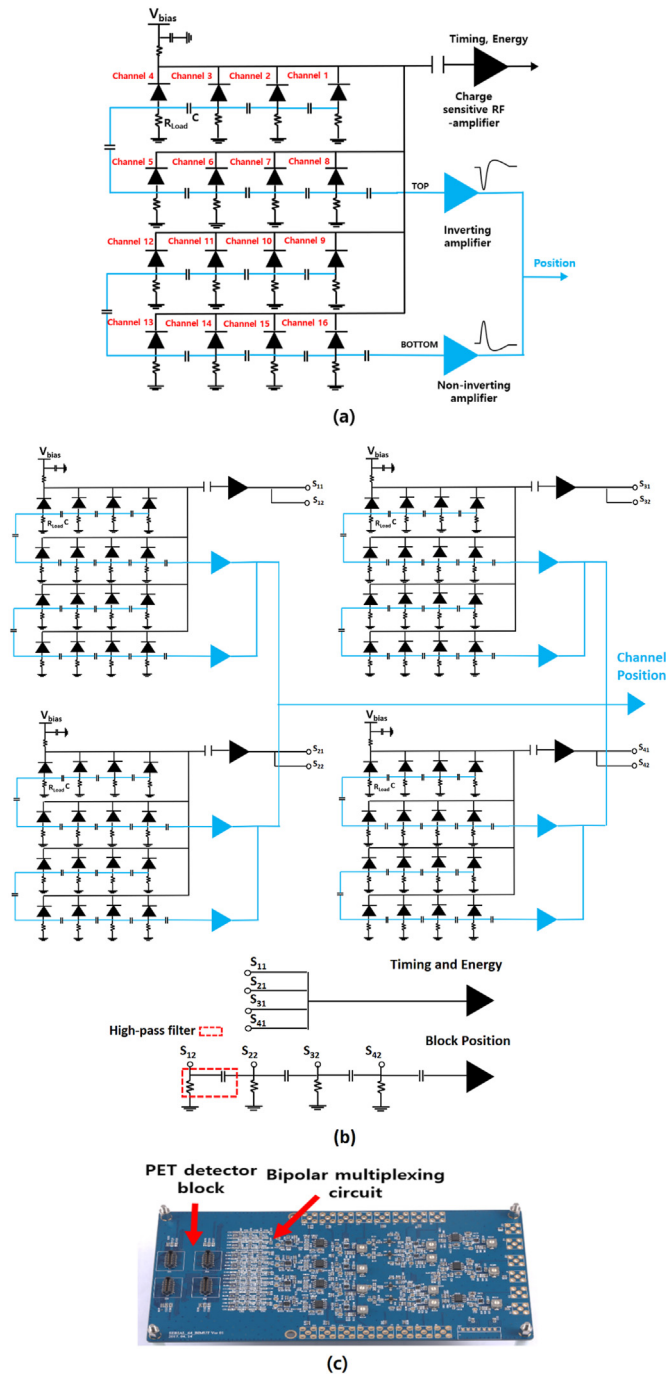### 2.3. Design of the serial line multiplexing circuit

The serial line multiplexing circuit was designed to identify up to 64 channels by expanding the circuit that is used to discriminate 8-channels. The 8-channel serial line multiplexing circuit was designed using 8 series-connected HPFs with different time constant values at each channel position. The resistor and capacitor values of the HPF of each channel are summarized in Table 1.

The 16-channel multiplexing circuit, which was designed to reduce the number of readout channels of a detector consisting of 4×4 array SiPM, was composed of two 8-channel serial line multiplexing circuits that generated position signals with different polarities using inverting and non-inverting amplifiers. The multiplexing circuit is divided into two 8-channel circuits to reduce pulse pile-up and to improve the accuracy of position determination. The two 8-channel circuits have HPFs with different time constant values for each channel position and the eight HPFs of each 8-channel circuit are series-connected.

As shown in Fig. 2 (a), channels 1 to 8 were referred to as the top 8-channel circuit and channels 9 to 16 were known as the bottom 8-channel circuit. The method of discriminating between the 16-channels is performed in two steps. First, the two 8-channel circuits are distinguished by the signal polarity that is used. The top 8-channel circuit is connected to an inverting amplifier to output
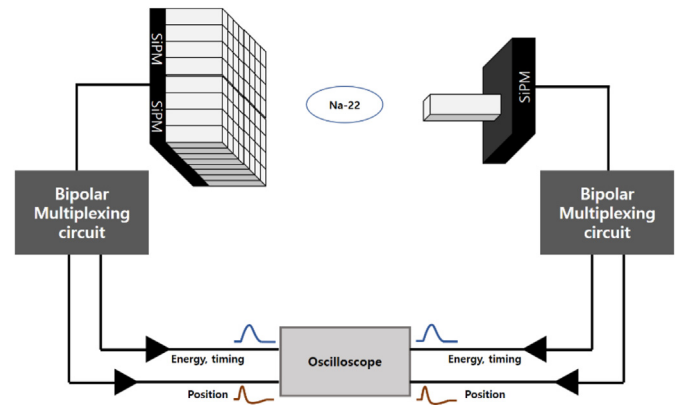

Fig. 1. An example of serial line multiplexing for 4 channels (a). Waveforms of the anode output pulse generated by the 4 different channel positions (b).

(a)

(b)

(c)

Fig. 2. Schematics of the 16-channel serial line multiplexing circuit (a) and 64-channel serial line multiplexing circuit (b). Image of the 64-channel serial line multiplexing board (c).

Fig. 3. Schematic diagram of the experimental setup used to obtain the position identification histogram, energy resolution and CRT.

four 16-channel multiplexing circuits were combined in parallel, and then sent to a current feedback amplifier circuit designed using a high slew rate operation amplifier (AD8000 CE, Analog devices, US) to identify the position of the detected gamma-ray signal. The four cathode summing output signals of the four 16-channel multiplexing circuits were individually amplified using a wideband RF-amplifier (MAR-3, mini-circuit, US) with a low input impedance and split into two signals each [27−29]. One of the two split signals from each detector block was combined without an additional filter in parallel to accurately measure energy and time information by minimizing distortion of the waveform of the summed signal. The other signal was combined through the HPF to identify the positions of the four detector blocks. The two combined signals were individually amplified using a high slew rate operation amplifier.

To examine the performance of the serial line multiplexing circuit according to the analog to digital converter (ADC) sampling rate, three amplified output signals from the serial line multiplexing circuit were digitized using a digital oscilloscope with a sampling rate of 10 GSPS and a data acquisition (DAQ) board consisting of an ADC with a sampling rate of 100 MSPS and FPGA (VHS-ADC, Lyrtech, Canada). The position, time, and energy information of the detected gamma-ray were measured using the digitized signals.

2.4. Performance evaluation: position identification histogram, energy resolution and coincidence resolving time

A detector block was fabricated using a 4×4 array of $3 \times 3 \times 20$ mm^3 LYSO crystals (Sinoceramics, Inc. China) and a 4×4 array of 3×3 mm^3 SiPM with a microcell size of 50 μm (S12642−050CN, Hamamatsu Photonics K·K. Japan). The LYSO crystals were polished on all sides and an additional reflector material (BaSO$_4$) was inserted between the array elements to increase the reflectivity of the array. The crystal array was coupled one-to-one with individual pixels of the SiPM using optical grease (BC-630, Saint-Gobain, France).

Fig. 3 shows a schematic diagram of the experimental setup that was used to record the position identification histogram, CRT and energy resolution. The CRT and energy resolution were measured according to the capacitance of the capacitor connecting the cathode summing output to the RF-amplifier in order to obtain the best performance from the serial line multiplexing circuit. The CRT was calculated using coincidence data by applying an energy window of 450−650 keV.

The zero-crossing point can be changed according to the amplitude of the anode summing output signal; however, this can

polarity-reversed waveforms, while the bottom 8-channel circuit is connected to a non-inverting amplifier to output regular waveforms. Second, the width of the bipolar pulse, from its rising edge to its zero-crossing position, was measured to identify the detected channel among the 8 channels. The two outputs from the two 8-channel circuits were combined to reduce the number of output channels to one anode summing output for position identification.

As shown in Fig. 2 (b) and (c), the 64-channel multiplexing circuit was designed based on the 16-channel multiplexing circuit described above. The four anode summing output signals of the

cause an error in the detected position. Therefore, to examine the error of the zero-crossing point value according to the amplitude in the same channel, the error was estimated as follows:

$$E_{zero-crossing\ point} = \frac{1}{n} \sum_{1}^{n} [Avg - P_n] \qquad (2)$$

where Avg is the average zero-crossing point value and P_n is the value of the nth zero-crossing point.

The detected position information was obtained by measuring the zero-crossing point of the anode summing output signal using the DAQ board and the digital oscilloscope. When acquiring data using a DAQ board, the error in the zero-crossing point measurement can increase due to the low sampling rate (100 MSPS) of the DAQ board. Linear interpolation was applied to the interval adjacent to the zero-crossing point among the falling time parts of the output signal to improve the accuracy of position identification. The position identification error was estimated by calculating the ratio of the overlapping area between two adjacent Gaussian fitted curves to the total area of each Gaussian fitted curve. The energy information of the detected signal was measured using the peak amplitude of the cathode summing output signal. The pulse data was acquired over 10k counts to reduce the statistical uncertainty (<1%).

2.5. Experimental setup of the proof-of-concept PET system

As shown in Fig. 4, the experimental setup of the proof-of-concept PET system consisted of a pair of four detector blocks with dimensions of 120 mm in diameter and 27 mm in height. A ^{22}Na point source with an activity of 598 kBq was located at the center of the field of view and 10 mm off-center, respectively. To evaluate the imaging capability of the proof-of-concept PET system, data were acquired in a step-and-shoot mode for 3 min per step, with a total of 36 steps over 180°. The point source image was reconstructed using a 2D filtered back-projection (FBP), using a Hann filter with a cutoff at the Nyquist frequency of 0.5.

3. Results

3.1. Measurement of the bipolar pulse waveform at 16 different positions through simulation and the serial line multiplexing circuit

Fig. 5 (a) and (b) show the simulation results of 16 channels with different RC time constant values, which demonstrate that all 16 channels were clearly identified. Fig. 5 (c) and (d) show the experimentally measured output pulses using the detector and the
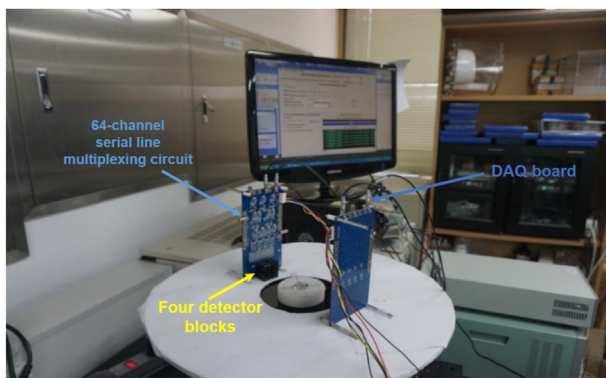

Fig. 4. Experimental setup used to examine the performance of the proof-of-concept PET system through the serial line multiplexing method.

measured pulse waveform obtained using the serial line multiplexing circuit, which were similar to those trends in the simulation results shown in Fig. 5 (a) and (b). The measured pulse output from the 16 channels can clearly be identified and the average position discrimination error was 5.2 ± 0.8%.

3.2. Bipolar pulse waveforms with different amplitudes in the same channel

Fig. 6 shows the measurement error of the zero-crossing point according to the amplitude of the signal output from a single channel measured using the digital oscilloscope and DAQ board. The error of the zero-crossing point of 9.6 ± 4.1% and 10.8 ± 3.2% were observed using the digital oscilloscope and DAQ board, respectively.

3.3. Position identification

Fig. 7 shows the 16-channel position identification histogram created using data obtained from the anode summing output with the digital oscilloscope and DAQ board. A representative position identification histogram from among those obtained with the four detector blocks is shown. The peak positions of the 16-channel position identification histograms were fitted with Gaussian curves. The approach of applying different RC time constant values results in more accurate position identification than the approach of applying the same RC time constant values. Therefore, only the experimental results recorded using the approach of applying different RC time constant values are presented. The use of the digital oscilloscope resulted in an error rate of 5.2 ± 0.8% (Fig. 7 (a) and (b)), while the use of the DAQ board resulted in an error rate of 7 ± 3.5% (Fig. 7 (c) and (d)).

As shown in Fig. 8 (a), the cathode summing output signal of each detector block has different zero-crossing point values, allowing us to identify the active detector block among the four detector blocks. Fig. 8 (b) shows the detector block discrimination histogram obtained by measuring the cathode summing output signal using the DAQ board. The four detector blocks can be clearly discriminated.

3.4. Energy spectra and CRT

The CRT and energy resolution varied depending on the capacitance of the capacitor connecting the cathode summing output signal to the RF-amplifier. Table 2 shows the CRT and energy resolution according to the capacitance (100 pF, 1 nF, 47 nF, 100 nF, and 470 nF) of the capacitor connecting the cathode summing output to the RF-amplifier. The best CRT performance was obtained when the capacitance was 100 pF, but the energy resolution deteriorated at that point. On the other hand, when the capacitance was 470 nF, the CRT performance deteriorated, but the best energy resolution was obtained. To reduce statistical uncertainty, CRT and energy resolution were measured at least 3 times for each value of capacitance.

Fig. 9 (a) and (b) show the time spectrum and energy spectra, respectively, obtained using the serial line multiplexing circuit approach (overvoltage = 2.0 V) approach while applying different RC time constant values using the digital oscilloscope. The average CRT of 580 ± 12 ps FWHM and average energy resolution of 13.2 ± 1.1% were measured with the detector block when the capacitance of the capacitor connecting the cathode summing output to the RF-amplifier was 100 nF"
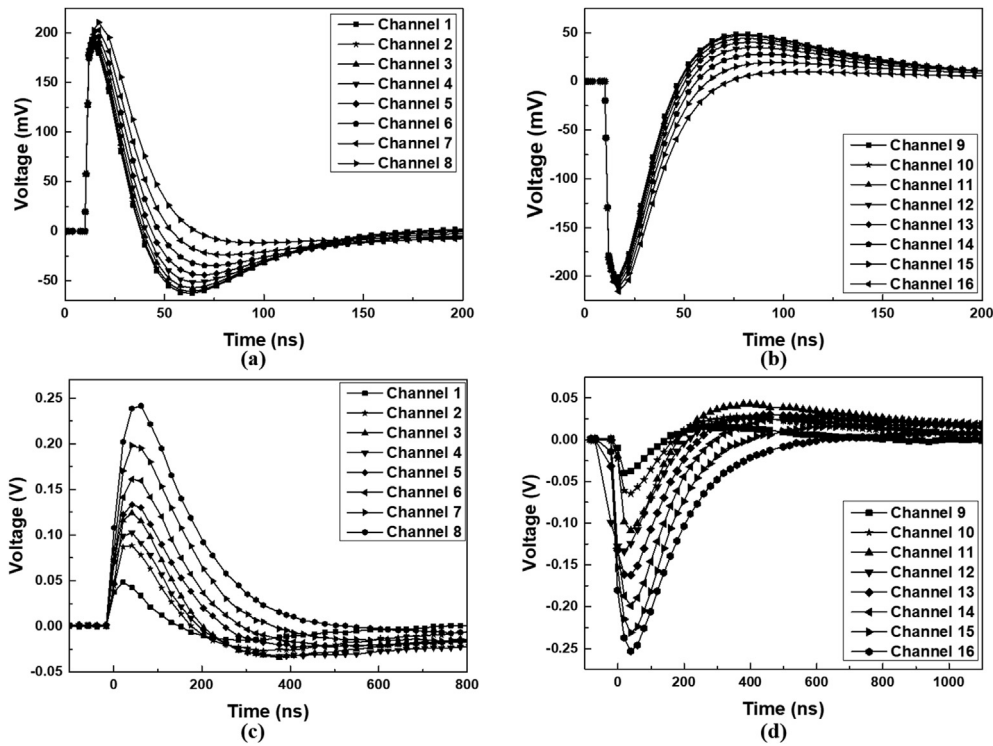
Fig. 5. Simulated bipolar signals from 16 different channels (a) and (b). Experimentally measured bipolar signals from 16 different channels (c) and (d) obtained using the serial line multiplexing circuit.
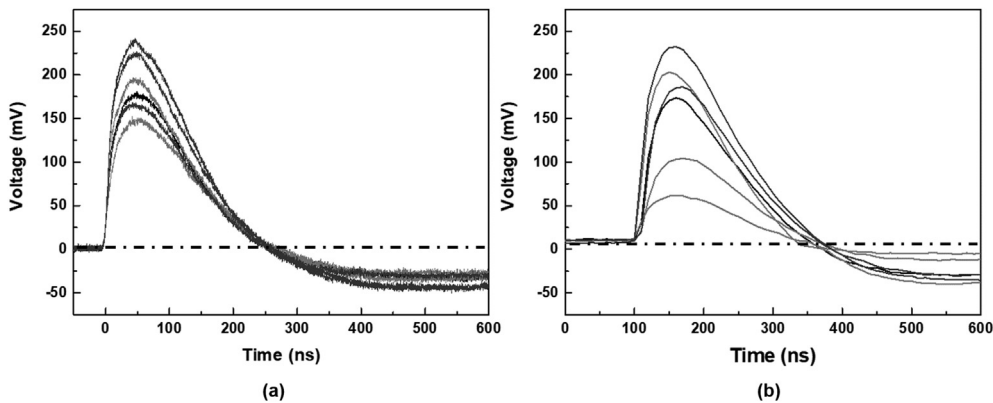

Fig. 6. Bipolar pulse waveforms generated with different detected signal amplitudes from the same channel, acquired using the digital oscilloscope (a) and the DAQ board (b).

3.5. Reconstructed imaging of proof-of-concept PET system using the serial line multiplexing method

The point source could be clearly resolved in the reconstructed image (Fig. 10). The radial resolution was 3.2 mm FWHM at the center of the field of view and 3.3 mm FWHM at 10 mm off-center.

4. Discussion

In this study, we proposed a novel multiplexing method that effectively reduces the number of readout channels while maintaining accurate position identification capability with good energy and timing performance. The serial line multiplexing method could achieve high channel reduction ratio and comparable energy and timing resolutions compared to charge division multiplexing

method [17,18,30]. Additionally, it could provide a more accurate position discrimination result than the multiplexing method utilizing an electrical delay line [19,20].

A simulation was performed to verify the principles of the proposed serial line multiplexing method and to derive a formula for determining the time constant of the high-pass filter (HPF). A series of experiments were also conducted to demonstrate the applicability of the proposed method in PET detectors with efficient channel multiplexing.

As shown in Table 2, a capacitance of 100 nF provided good energy performance while preserving moderate CRT performance. The trade-off between CRT and energy resolution depending on the capacitance should be considered in order to achieve the best performance of the multiplexing circuit. This is because the amplitude and rise time of the signals are affected by the
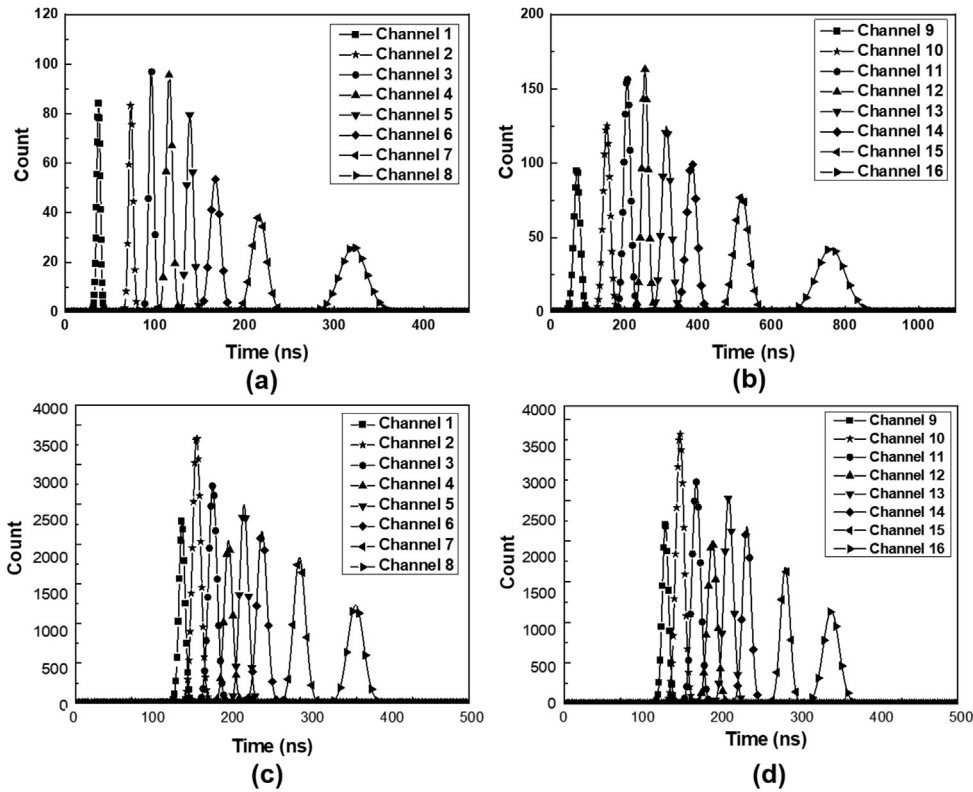
Fig. 7. Position identification histogram for channels 1–8 (left) and 9–16 (right) measured using the digital oscilloscope (a) and (b) and DAQ board (c) and (d).
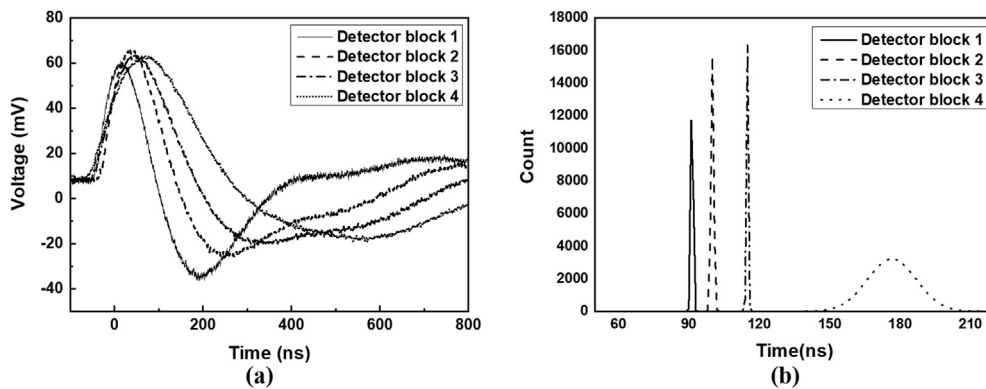

Fig. 8. Experimentally measured bipolar signals from the 4 different detector blocks obtained using the serial line multiplexing circuit (a). Position identification spectrum of detector blocks 1–4 obtained by measuring zero-crossing points for detector blocks (b).

Table 2
CRT and energy resolution as a function of the capacitance of the capacitor connecting the cathode summing output to the RF-amplifier.

Capacitor value (nF)	Energy resolution (% FWHM)	CRT (ps FWHM)
0.1	19.8 ± 0.5	483 ± 7.3
1	16.4 ± 1.5	521 ± 9.3
47	14.3 ± 1.8	567 ± 7.5
100	13.2 ± 1.1	580 ± 12
470	9.5 ± 0.8	637 ± 10.2

capacitance of the capacitor connecting the cathode summing output to the RF-amplifier. A smaller capacitance, which provides a faster rise time, has a positive effect on the timing performance.

However, it degrades energy resolution because the amplitude of the cathode summing output signal is reduced. The timing performance of the proposed method is relatively low because the noise of each cathode channel is accumulated in the cathode summing output signal. Additionally, it should be noted that the proposed method can only be employed with a detector that uses one-to-one coupling between the crystal elements and photosensor pixel.

As illustrated in Fig. 5, the simulation results showed that the output pulses of channels 1 to 8 and 9 to 16 had similar pulse shapes despite their opposite polarities. The shape of the output pulses from channels 1–8 and 9–16, which were experimentally
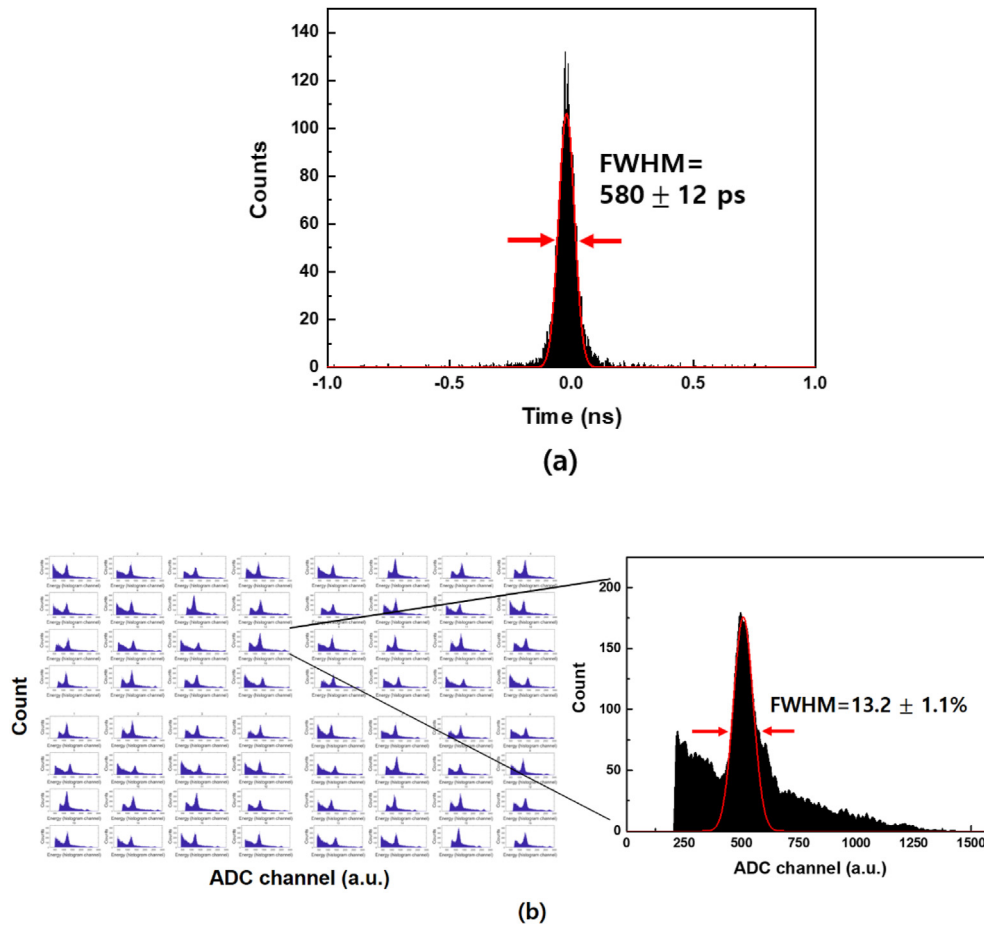
Fig. 9. Representative coincidence time spectrum (a) and energy spectra of 64 channels (b) obtained with the serial line multiplexing circuit.
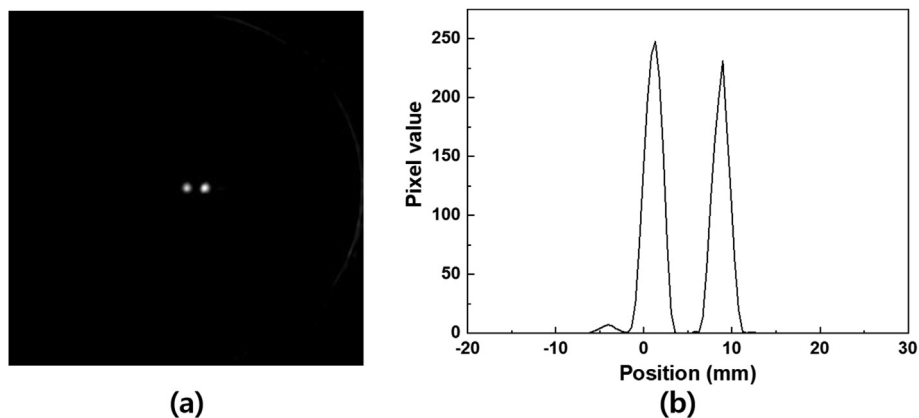

Fig. 10. The reconstructed image and line profiles acquired using the proof-of-concept PET system.

measured using the detector block, differed slightly due to differences in input impedance between the inverting and noninverting amplifiers. However, the shape of the output pulses and the interval between the important zero-crossing values were fundamentally similar.

As shown in Fig. 6, the error of the zero-crossing point values according to the amplitude of the signal output from a single channel was less than 5%. Therefore, the output signal at the same position was not affected by the amplitude, and accurate position

identification results could be achieved regardless of the magnitudes of the detected signals.

The errors in position identification measured by the method that used the same RC time constant were similar to those of the method that used different RC time constants. However, the approach of applying the same RC time constant could cause a dead time problem because the length of the output signal increased as the number of channels increased. The accuracy of position identification depended on the ADC sampling rate, but the difference

between the position identification error obtained using the DAQ board and the digital oscilloscope was relatively small (7 ± 3.5%), indicating that the use of a general DAQ does not significantly affect the position identification performance.

A point source image was successfully acquired using the proof-of-concept PET system with the serial line multiplexing method. This result demonstrated the imaging capability of the proposed multiplexing method with a high multiplexing ratio.

5. Conclusion

A serial line multiplexing circuit was developed and its applicability to a PET system was evaluated. The experimental results validated the serial line multiplexing method, which reduced the number of data acquisition channels at a 64:3 ratio. The results also showed that distinct crystal identification could be performed based on the zero-crossing point difference between bipolar pulse signals. The serial line multiplexing method could provide a high channel reduction ratio and perform simple position identification by measuring the zero-crossing point of the output signal without using an algorithm for position identification. This simplicity is in contrast to the complexity of conventional charge division methods. Additionally, the proposed method could easily be extended to circuits with high channel reduction rates, such as 128:3 or 256:3, thus reducing the system development cost and complexity of various gamma-ray imaging systems, including gamma cameras and SPECT as well as PET.

Declaration of competing interest

The authors declare that they have no known competing financial interests or personal relationships that could have appeared to influence the work reported in this paper.

Acknowledgments

References

[1] A.L. Goertzen, X. Zhang, M.M. McClarty, E.J. Berg, C.Y. Liu, P. Kozlowski, F. Retiere, L. Ryner, V. Sossi, G. Stortz, C.J. Thompson, Design and performance of a resistor multiplexing readout circuit for a SiPM detector, IEEE Trans. Nucl. Sci. 60 (2013) 1541−1549, https://doi.org/10.1109/TNS.2013.2251661.

[2] J.H. Jung, Y. Choi, K.J. Hong, W. Hu, J. Kang, B.J. Min, S.H. Shin, H.K. Lim, Y. Huh, E.-J. Kim, Development of a position decoder circuit for PET consisting of GAPD arrays, Nucl. Instrum. Methods Phys. Res. Sect. A Accel. Spectrom. Detect. Assoc. Equip. 621 (2010) 310−315, https://doi.org/10.1016/j.nima.2010.04.028.

[3] K.J. Hong, Y. Choi, J.H. Jung, J. Kang, W. Hu, H.K. Lim, Y. Huh, S. Kim, J.W. Jung, K.B. Kim, M.S. Song, H.-W. Park, A prototype MR insertable brain PET using tileable GAPD arrays, Med. Phys. 40 (2013), 042503, https://doi.org/10.1118/1.4793754.

[4] S. Lee, Y. Choi, J. Kang, J.H. Jung, Development of a multiplexed readout with high position resolution for positron emission tomography, Nucl. Instrum. Methods Phys. Res. Sect. A Accel. Spectrom. Detect. Assoc. Equip. 850 (2017) 42−47, https://doi.org/10.1016/j.nima.2017.01.026.

[5] M.F. Bieniosek, J.W. Cates, C.S. Levin, Achieving fast timing performance with multiplexed SiPMs, Phys. Med. Biol. 61 (2016) 2879−2892, https://doi.org/10.1088/0031-9155/61/7/2879.

[6] M.F. Bieniosek, J.W. Cates, A.M. Grant, C.S. Levin, Analog filtering methods improve leading edge timing performance of multiplexed SiPMs, Phys. Med. Biol. 61 (2016), https://doi.org/10.1088/0031-9155/61/16/N427.

[7] I. Kwon, T. Kang, M.D. Hammig, Experimental validation of charge-sensitive amplifier configuration that compensates for detector capacitance, IEEE Trans. Nucl. Sci. 63 (2016) 1202−1208, https://doi.org/10.1109/TNS.2016.2530065.

[8] S. Siegel, R.W. Silverman, S.R. Cherry, E. Shao, Simple charge division readouts for imaging scintillator arrays using a multi-channel, 1995, IEEE Nucl. Sci. Symp. Med. Imaging Conf. Rec. 1 (1995) 13−17, https://doi.org/10.1109/NSSMIC.1995.504167.

[9] P.D. Olcott, J.A. Talcott, C.S. Levin, F. Habte, A.M.K. Foudray, Compact readout electronics for position sensitive photomultiplier tubes, IEEE Trans. Nucl. Sci. 52 (2005) 21−27, https://doi.org/10.1109/TNS.2004.843134.

[10] D. Stratos, G. Maria, F. Eleftherios, L. George, Comparison of three resistor network division circuits for the readout of 4 x 4 pixel SiPM arrays, Nucl. Instrum. Methods Phys. Res. Sect. A Accel. Spectrom. Detect. Assoc. Equip. 702 (2013) 121−125, https://doi.org/10.1016/j.nima.2012.08.006.

[11] D. Kim, C.-H. Kim, I. Kwon, Experimental results on a detector capacitance compensation technique for multiplexing SiPM channels, Nucl. Instrum. Methods Phys. Res. Sect. A Accel. Spectrom. Detect. Assoc. Equip. 954 (2020) 161527, https://doi.org/10.1016/j.nima.2018.10.205.

[12] I. Kwon, T. Kang, B.T. Wells, L.J. D'Aries, M.D. Hammig, Compensation of the detector capacitance presented to charge-sensitive preamplifiers using the Miller effect, Nucl. Instrum. Methods Phys. Res. Sect. A Accel. Spectrom. Detect. Assoc. Equip. 784 (2015) 220−225, https://doi.org/10.1016/j.nima.2014.12.049.

[13] E. Downie, X. Yang, H. Peng, Investigation of analog charge multiplexing schemes for SiPM based PET block detectors, Phys. Med. Biol. 58 (2013) 3943−3964, https://doi.org/10.1088/0031-9155/58/11/3943.

[14] J. Du, J.P. Schmall, Y. Yang, K. Di, P.A. Dokhale, K.S. Shah, S.R. Cherry, A simple capacitive charge-division readout for position-sensitive solid-state photo-multiplier arrays, IEEE Trans. Nucl. Sci. 60 (2013) 3188−3197, https://doi.org/10.1109/TNS.2013.2275012.

[15] H. Choe, Y. Choi, W. Hu, J. Yan, J.H. Jung, Development of capacitive multiplexing circuit for SiPM-based time-of-flight (TOF) PET detector, Phys. Med. Biol. 62 (2017) N120−N133, https://doi.org/10.1088/1361-6560/aa5f9b.

[16] H. Park, G.B. Ko, J.S. Lee, Hybrid charge division multiplexing method for silicon photomultiplier based PET detectors, Phys. Med. Biol. 62 (2017) 4390−4405, https://doi.org/10.1088/1361-6560/aa6aea.

[17] X. Sun, K. Lou, Y. Shao, Capacitor based multiplexing circuit for silicon photomultiplier array readout. IEEE Nucl. Sci. Symp. Med. Imaging Conf., IEEE, 2014, pp. 1−5.

[18] Z. Wang, X. Sun, K. Lou, J. Meier, R. Zhou, C. Yang, X. Zhu, Y. Shao, Design, development and evaluation of a resistor-based multiplexing circuit for a 20×20 SiPM array, Nucl. Instrum. Methods Phys. Res. Sect. A Accel. Spectrom. Detect. Assoc. Equip. 816 (2016) 40−46, https://doi.org/10.1016/j.nima.2016.01.081.

[19] R. Vinke, J.Y. Yeom, C.S. Levin, Electrical delay line multiplexing for pulsed mode radiation detectors, Phys. Med. Biol. 60 (2015) 2785−2802, https://doi.org/10.1088/0031-9155/60/7/2785.

[20] H. Kim, C.-T. Chen, N. Eclov, A. Ronzhin, P. Murat, E. Ramberg, S. Los, C.-M. Kao, A silicon photo-multiplier signal readout using strip-line and waveform sampling for Positron Emission Tomography, Nucl. Instrum. Methods Phys. Res. Sect. A Accel. Spectrom. Detect. Assoc. Equip. 830 (2016) 119−129, https://doi.org/10.1016/j.nima.2016.05.085.

[21] K.B. Kim, H.T. Leem, Y.H. Chung, H.-B. Shin, Feasibility study of multiplexing method using digital signal encoding technique, J Nucl Eng Technol 52 (2020) 2339−2345, https://doi.org/10.1016/j.net.2020.03.027.

[22] J.Y. Won, G.B. Ko, J.S. Lee, Delay grid multiplexing: simple time-based multiplexing and readout method for silicon photomultipliers, Phys. Med. Biol. 61 (2016) 7113−7135, https://doi.org/10.1088/0031-9155/61/19/7113.

[23] F. Villa, Y. Zou, A. Dalla Mora, A. Tosi, F. Zappa, SPICE electrical models and simulations of silicon photomultipliers, IEEE Trans. Nucl. Sci. 62 (2015) 1950−1960, https://doi.org/10.1109/TNS.2015.2477716.

[24] K.B. Kim, Y. Choi, J. Kang, J.H. Jung, W. Hu, Signal transmission with long cable for design of PET detector for hybrid PET-MRI, IEEE Trans. Nucl. Sci. 62 (2015) 2010−2016, https://doi.org/10.1109/TNS.2015.2462730.

[25] F. Corsi, C. Marzocca, A. Perrotta, A. Dragone, M. Foresta, A. Del Guerra, S. Marcatili, G. Llosa, G. Collazzuol, G.F. Dalla Betta, N. Dinu, C. Piemonte, G.U. Pignatel, G. Levi, Electrical characterization of silicon photo-multiplier detectors for optimal front-end design, IEEE Nucl. Sci. Symp. Conf. Rec. 2 (2007) 1276−1280, https://doi.org/10.1109/NSSMIC.2006.356076.

[26] SensL, Readout Methods for Arrays of SiPM, 2014, pp. 1−15. SensL.

[27] P. Avella, A. De Santo, A. Lohstroh, M.T. Sajjad, P.J. Sellin, A study of timing properties of silicon photomultipliers, Nucl. Instrum. Methods Phys. Res. Sect. A Accel. Spectrom. Detect. Assoc. Equip. 695 (2012) 257−260, https://doi.org/10.1016/j.nima.2011.11.049.

[28] K.B. Kim, Y. Choi, J. Jung, S. Lee, H. jun Choe, H.T. Leem, Analog and digital signal processing method using multi-time-over-threshold and FPGA for PET, Med. Phys. 45 (2018) 4104−4111, https://doi.org/10.1002/mp.13101.

[29] J.Y. Yeom, R. Vinke, C.S. Levin, Optimizing timing performance of silicon photomultiplier based scintillation detectors, IEEE Nucl. Sci. Symp. Conf. Rec. 58 (2012) 3119−3121, https://doi.org/10.1109/NSSMIC.2012.6551711.

[30] H. Choe, Y. Choi, D.J. Kwak, J. Lee, Prototype time-of-flight PET utilizing capacitive multiplexing readout method, Nucl. Instrum. Methods Phys. Res. Sect. A Accel. Spectrom. Detect. Assoc. Equip. 921 (2019) 43−49, https://doi.org/10.1016/j.nima.2018.12.030.